

# Synthesis, Photophysical Characterization, and Surface Photovoltage Spectra of Windmill-Shaped Phthalocyanine–Porphyrin Heterodimers and Heteropentamers

Zhixin Zhao,<sup>[a]</sup> Chun-Ting Poon,<sup>[a]</sup> Wai-Kwok Wong,<sup>\*[a]</sup> Wai-Yeung Wong,<sup>[a]</sup>  
Hoi-Lam Tam,<sup>[b]</sup> Kok-Wai Cheah,<sup>[b]</sup> Tengfeng Xie,<sup>[c]</sup> and Dejun Wang<sup>[c]</sup>

**Keywords:** Energy transfer / Photoluminescence / Photovoltage spectra / Phthalocyanines / Porphyrins

The synthesis and characterization of three nonperipherally substituted, covalently-linked phthalocyanine–porphyrin hybrid molecules is described. The optical and photophysical properties of these compounds are studied in detail. The intramolecular energy transfer process is investigated and quantified in terms of the quantum yield of the energy transfer and is found to be highly effective in these molecules.

The photophysical properties of the phthalocyanine core of these three compounds are significantly modified by the presence of the porphyrin moieties. These molecules display interesting optical-power-limiting behavior and a surface photovoltaic effect.

(© Wiley-VCH Verlag GmbH & Co. KGaA, 69451 Weinheim, Germany, 2008)

## Introduction

The chemistry of light-harvesting and energy-transferring molecular arrays has attracted a lot of attention over the years because of the ability of these systems to mimic the function of chlorophyll in plants during photosynthesis.<sup>[1]</sup> As a light-harvesting system, they should be able to capture solar energy over a broad spectral range and channel the energy swiftly for use in chemical reactions. The ability of undergoing excited-state energy transfer is an important prerequisite for a good molecular photonic device. Phthalocyanines are an important class of organic compounds, which have many applications as xerographic photoreceptors,<sup>[2]</sup> as optical recording,<sup>[3]</sup> infrared sensors,<sup>[4]</sup> and organic photoelectronic devices,<sup>[5]</sup> and as a photosensitizer in the photodynamic therapy (PDT) of cancer.<sup>[6]</sup> Phthalocyanines are 18- $\pi$ -electron aromatic compounds that comprise four isoindoles. Two-dimensional aromatic delocalization over these macrocycles gives rise to their exceptional optical and electrical properties. Phthalocyanines are generally stable, rigid compounds with varying properties that depend upon their central metals, and peripheral and axial substituents. Porphyrin–phthalocyanine arrays

are ideal candidates for application in light-harvesting and molecular photonics. Porphyrins and phthalocyanines represent two related classes of very versatile macrocyclic organic molecules and typically display complementary optical properties. Phthalocyanines have two absorption bands, a strong Q band in the red region (600–700 nm) and a medium-strength Soret band in the UV range (350 nm), whereas porphyrins have a strong B band in the region 410–430 nm and medium-strength Q bands between 510 and 650 nm. Their ground-state absorptions cover the entire visible region of the spectrum. The first synthesis of a porphyrin–phthalocyanine conjugate, a dimer from a zinc porphyrin and a zinc phthalocyanine, was reported about two decades ago by Gaspard et al.,<sup>[7]</sup> with the ultimate aim of investigating their photochemical properties. A few papers have also appeared in recent years in which the authors reported on investigations to exploit the electronic- and photonic-based cooperation between individual subunits of porphyrins and phthalocyanines.<sup>[8,9]</sup>

The efficiency of intramolecular electron- and energy transfer processes in oxygen-linked chromophores is of interest as they are suitable as model systems for photosynthesis. Recently, the synthesis and photophysical properties of a trimer, pentamer, and nanomer, in which a phthalocyanine molecule was connected by an ether linkage to two, four, and eight porphyrin molecules, respectively, and their transition-metal [Zn<sup>II</sup> and Co<sup>II</sup>] complexes were reported.<sup>[10]</sup> In this paper, we report the synthesis, photophysical, and surface photovoltage properties of nonperipherally-substituted windmill phthalocyanine–porphyrin heterodimers and heteropentamers.

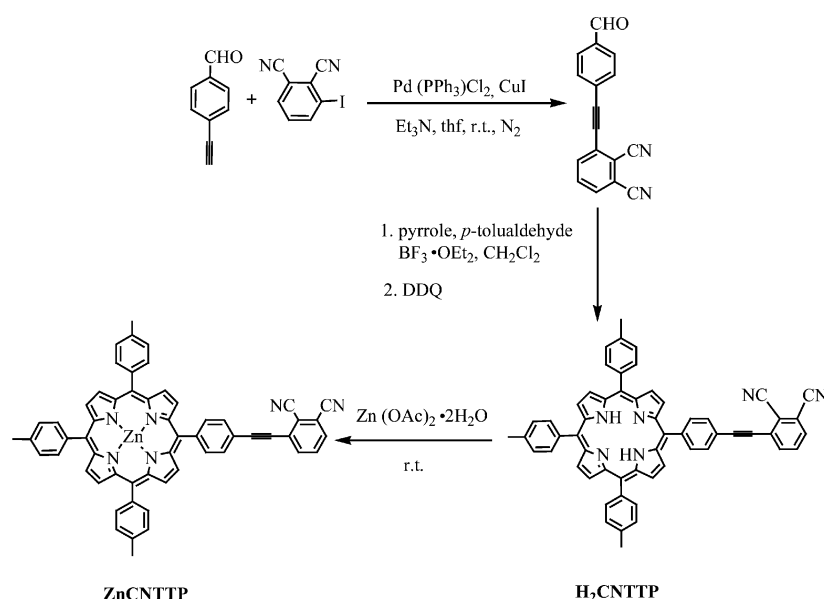
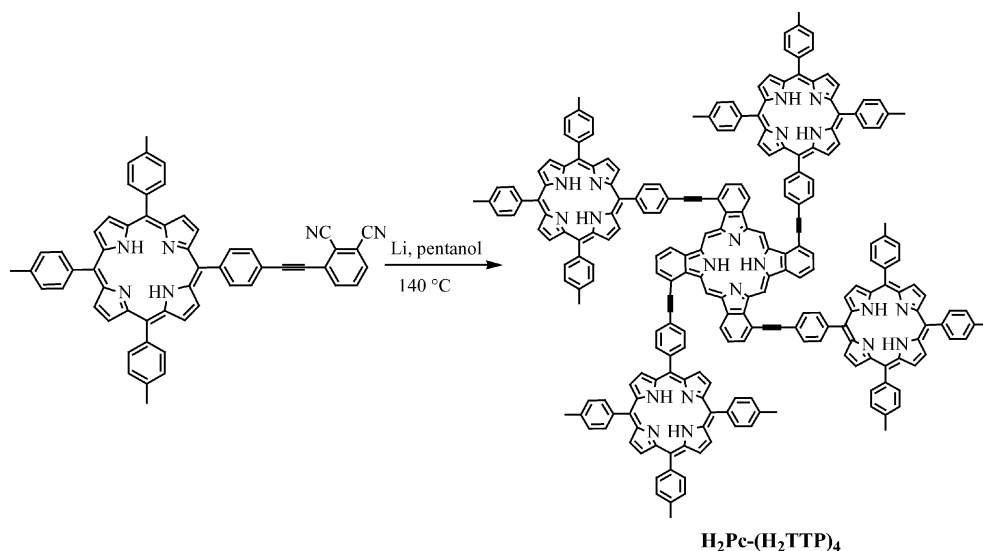
[a] Department of Chemistry and Centre for Advanced Luminescence Materials, Hong Kong Baptist University, Waterloo Road, Hong Kong, P. R. China  
Fax: +852-3411-7348  
E-mail: wkwong@hkbu.edu.hk

[b] Department of Physics and Centre for Advanced Luminescence Materials, Hong Kong Baptist University, Waterloo Road, Hong Kong, P. R. China

[c] College of Chemistry, Jilin University, 2699 Qianjin Street, Changchun, 130012, P.R. China

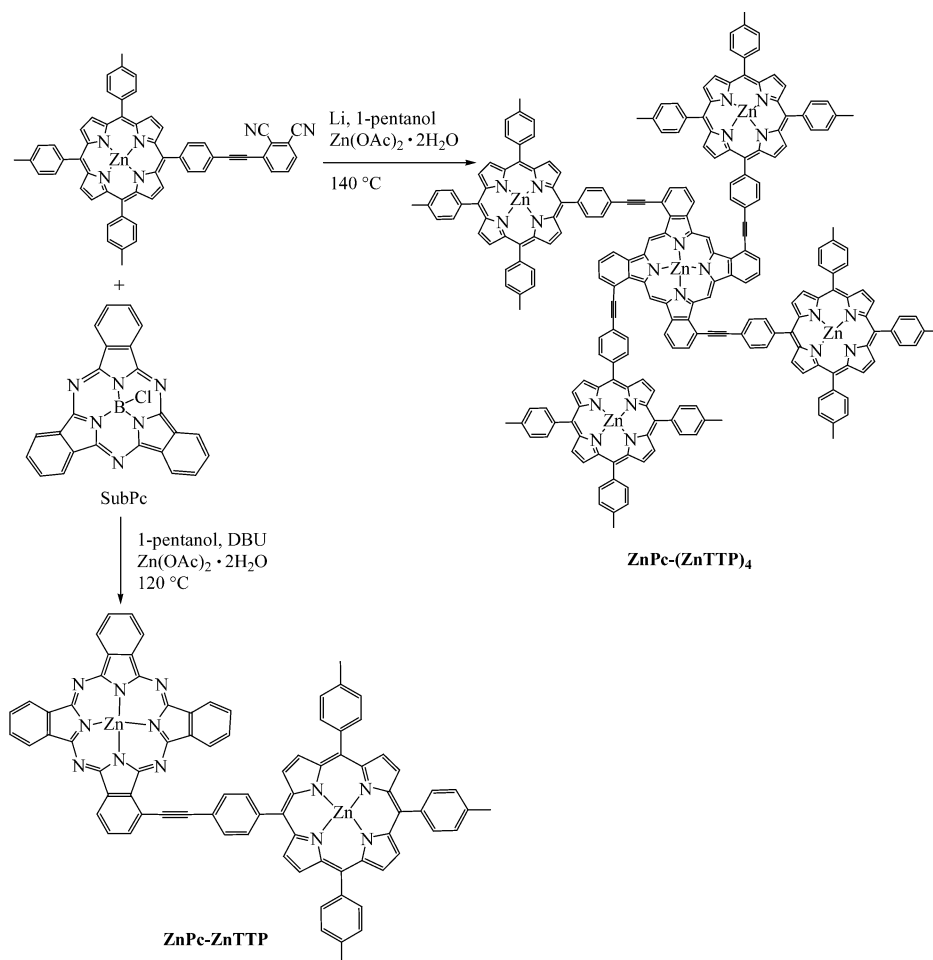
## Synthesis and Characterization

tion of phthalonitrile–benzaldehyde, *p*-tolualdehyde, and pyrrole in CH<sub>2</sub>Cl<sub>2</sub> in the presence of BF<sub>3</sub>·OEt<sub>2</sub> at room temperature followed by oxidation with 2,3-dichloro-5,6-dicyano-1,4-benzoquinone (DDQ) afforded a mixture of porphyrins. Because the porphyrins bear different numbers of polar groups, the desired ethynyl-linked porphyrin–phthalonitrile (H<sub>2</sub>CNTTP) was easily isolated in 15% yield after two flash silica gel columns in which CHCl<sub>3</sub>/hexane (3:1, v/v) was the eluent (Scheme 1). The UV/Vis absorption spectrum of H<sub>2</sub>CNTTP, which displays a Soret band at 422 nm and Q bands at 517, 552, 593, and 649 nm, is typical of normal porphyrin-free bases. H<sub>2</sub>CNTTP exhibits the [M + 1]<sup>+</sup> peak at *m/z* = 807.3262, which is in good agreement with the theoretical value of 807.3231, in its MALDI-TOF mass spectrum, a singlet at  $\delta$  = −2.78 ppm for the inner NH protons of the porphyrin in its <sup>1</sup>H NMR spectrum.

Scheme 1. Synthesis of H<sub>2</sub>CNTTP and ZnCNTTP.Scheme 2. Synthesis of H<sub>2</sub>Pc-(H<sub>2</sub>TTP)<sub>4</sub>.

and an N–H and C≡N stretch at 3316 and 2217 cm<sup>−1</sup>, respectively, in its IR spectrum. The Zn<sup>II</sup> metalloporphyrin could be prepared quantitatively by refluxing the porphyrin-free base with an equivalent amount of hydrated zinc acetate in a CHCl<sub>3</sub>/methanol mixture. The Zn<sup>II</sup> complex, ZnCNTTP, displays an electronic absorption spectrum characteristic of normal metalloporphyrin complexes with a Soret band at 426 nm and two Q bands at 551 and 591 nm. The formation of the metalloporphyrin ZnCNTTP was further confirmed by the disappearance of the inner NH resonance in the <sup>1</sup>H NMR spectrum and the N–H stretch in the IR spectrum. The IR spectrum of the complex exhibits a C≡N stretch at 2217 cm<sup>−1</sup>. The MALDI-TOF mass spectrum of ZnCNTTP also exhibits the [M + 1]<sup>+</sup> peak at *m/z* = 868.2247, which agrees well with the theoretical value of 868.2292. The metal-free phthalocyanine–porphyrin conjugate H<sub>2</sub>Pc–(H<sub>2</sub>TTP)<sub>4</sub> was synthesized by cyclotetramerization of H<sub>2</sub>CNTTP by using the lithium pentoxide method (Scheme 2). The initial product of the lithium pentoxide method was dilithium phthalocyanine (Li<sub>2</sub>Pc), in which the lithium ions can readily be displaced by other transition-metal ions. Thus, the subsequent addition of metal salts to Li<sub>2</sub>Pc provides a convenient method for the

preparation of other metallophthalocyanines. Cyclotetramerization of ZnCNTTP with the addition of hydrated zinc acetate and after a heating period of 4 h afforded the all-zinc chelate ZnPc–(ZnTTP)<sub>4</sub> (Scheme 3). The free base and the metalated products are very stable in air and can easily be purified by silica gel column chromatography. When eluted with a CHCl<sub>3</sub>/methanol (50:1, v/v) mixture, a green-brown band was obtained from which the desired product was isolated. The formation of the phthalocyanine ring is characterized by the appearance of phthalocyanine Q bands in the electronic absorption spectrum. Thus, the presence of two Q band absorptions at 687 and 718 nm for H<sub>2</sub>Pc–(H<sub>2</sub>TTP)<sub>4</sub> and one Q band absorption at 695 nm for ZnPc–(ZnTTP)<sub>4</sub> confirms the formation of the phthalocyanine ring for the two compounds. The disappearance of the C≡N stretch in the IR spectrum of H<sub>2</sub>CNTTP and ZnCNTTP at 2217 and 2212 cm<sup>−1</sup>, respectively, further supports the cyclotetramerization of phthalonitrile to phthalocyanine. The MALDI-TOF mass spectra of the two compounds reveal the [M + 1]<sup>+</sup> peak at *m/z* = 3230.2765 and 3546.8359, which are in good agreement with the calculated values of 3230.2924 and 3546.8530 for H<sub>2</sub>Pc–(H<sub>2</sub>TTP)<sub>4</sub> and ZnPc–(ZnTTP)<sub>4</sub>, respectively.



Scheme 3. Synthesis of ZnPc–ZnTTP and ZnPc–(ZnTTP)<sub>4</sub>.

The unsymmetrical heterodimer ZnPc-ZnTTP was synthesized in satisfactory yield (28%) by condensation of ZnCNTTP (1 equiv.) with excess chloro[7,12:14,19-diimino-21,5-nitrilo-5*H*-tribenzo[*c,h,m*][1,6,11]triazacyclopentadecinato(2-)-κN<sup>22</sup>,κN<sup>23</sup>,κN<sup>24</sup>]boron(III) (SubPc, 5 equiv.) in the presence of hydrated zinc acetate (5 equiv.).<sup>[10b]</sup> The only by-product of the reaction was ZnPc, which could readily be separated from the desired product by column chromatography. The heterodimer ZnPc-ZnTTP could easily be eluted from a silica gel column, whereas the by-product ZnPc remained stationary on the top of the column when eluted with a mixture of dichloromethane/methanol (19:1, v/v). The MALDI-TOF mass spectrum of ZnPc-ZnTTP displays the [M]<sup>+</sup> peak at  $m/z = 1320.2721$ , which is in agreement with the theoretical value of 1320.2683. The appearance of the Q band at 676 nm in the UV/Vis absorption spectrum and the disappearance of the C≡N stretch at 2212 cm<sup>-1</sup> in the IR spectrum further supports the claim that the product is a phthalocyanine complex.

### Absorption Properties

The electronic absorption spectrum of the phthalocyanine–porphyrin conjugates is basically the sum of the absorption spectra of phthalocyanine and porphyrin moieties, with a slight bathochromic shift of the Q bands of the phthalocyanine moiety. Figure 1 shows the absorption spectra of H<sub>2</sub>TTP, H<sub>2</sub>Pc, and H<sub>2</sub>Pc-(H<sub>2</sub>TTP)<sub>4</sub> in CHCl<sub>3</sub>. The two Q bands assigned to the phthalocyanine moiety of H<sub>2</sub>Pc-(H<sub>2</sub>TTP)<sub>4</sub> at 687 and 718 nm are redshifted by 26–32 nm relative to those of H<sub>2</sub>Pc, which are at 655 and 692 nm, respectively. Such a bathochromic shift is probably attributed to the extension of the conjugated  $\pi$ -system involving the four phenylethynyl linkers from the attached porphyrins and the distortion of the planarity of the phthalocyanine ring. The zinc(II) complexes of the phthalocyanine–porphyrin conjugates display similar absorption behavior. Figure 2 shows the absorption spectra of ZnTTP, ZnPc, ZnPc-ZnTTP, and ZnPc-(ZnTTP)<sub>4</sub> in CHCl<sub>3</sub>. The phthalocyanine Q band for ZnPc at 671 nm is redshifted to 676 and 695 nm for ZnPc-ZnTTP and ZnPc-(ZnTTP)<sub>4</sub>, respectively. The bathochromic shift of the phthalocyanine Q band increases from 5 to 24 nm as the number of peripheral ZnTTP moieties attached to ZnPc increases from 1 to 4. It has been shown that the electron-donating substituents on metallophthalocyanine complexes give rise to red shifts in the Q band absorptions.<sup>[12]</sup> The shift in the Q band to longer wavelengths for the ZnPc moiety in the spectra of ZnPc-ZnTTP and ZnPc-(ZnTTP)<sub>4</sub> suggests that other than the extension of  $\pi$ -conjugation, peripheral ZnTTP substituents may also exert electron-donating effects on ZnPc. At high concentration, the absorbance of the phthalocyanine Q band of ZnPc-ZnTTP and ZnPc-(ZnTTP)<sub>4</sub> deviates from linearity, which indicates that aggregation might occur through the phthalocyanine moiety.

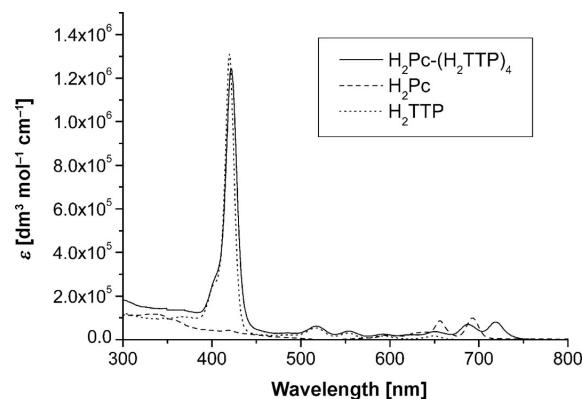


Figure 1. UV/Vis absorption spectra of H<sub>2</sub>TTP, H<sub>2</sub>Pc, and H<sub>2</sub>Pc-(H<sub>2</sub>TTP)<sub>4</sub> (approximately  $1.0 \times 10^{-6}$  M) in CHCl<sub>3</sub>.

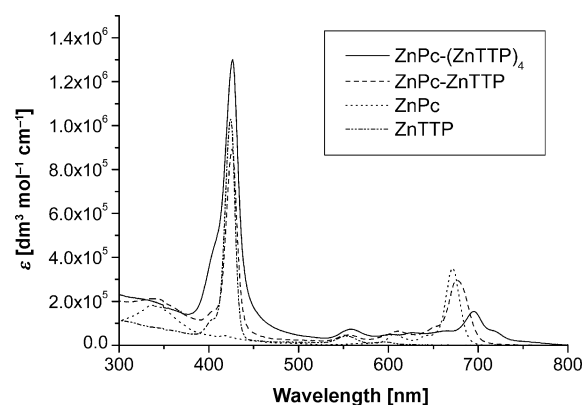


Figure 2. UV/Vis absorption spectra of ZnTTP, ZnPc, ZnPc-ZnTTP, and ZnPc-(ZnTTP)<sub>4</sub> (approximately  $1.0 \times 10^{-6}$  M) in CHCl<sub>3</sub>.

### Fluorescence Properties

The absorption, excitation, and fluorescence spectra of the three conjugated dyads H<sub>2</sub>Pc-(H<sub>2</sub>TTP)<sub>4</sub>, ZnPc-ZnTTP, and ZnPc-(ZnTTP)<sub>4</sub> are shown in Figures 3, 4, and 5, respectively. In each array, illumination of the porphyrin component results in fluorescence exclusively from the phthalocyanine moiety. For example, the fluorescence spectrum of H<sub>2</sub>Pc-(H<sub>2</sub>TTP)<sub>4</sub> (Figure 3) obtained by excitation at the Q band of the porphyrin moieties ( $\lambda_{\text{exc}} = 515$  nm) is essentially the same as that obtained when excitation was carried out at the Q band of the phthalocyanine moiety ( $\lambda_{\text{exc}} = 627$  nm). In the fluorescence spectrum, other than the phthalocyanine emission at  $\lambda_{\text{em}} = 720$  nm, which is redshifted by 23 nm relative to that of H<sub>2</sub>Pc ( $\lambda_{\text{em}} = 697$  nm), there is no evidence of any emission from the porphyrin moieties (expected fluorescence at 650 nm). These results indicate a very efficient photoinduced intramolecular energy transfer from the porphyrin to the phthalocyanine components in the pentamer. A similar photoluminescence behavior is also observed for the other two oligomers. The fluorescence band of ZnPc-ZnTTP and ZnPc-(ZnTTP)<sub>4</sub> relative to that of the ZnPc complex (675 nm) is redshifted by 11 and 29 nm to 687 and 704 nm, respectively. The excitation spectra (monitored at 800 nm) of the three dyads are

coincident with their ground-state absorption spectra (Figures 3–5) and reveal contribution of both phthalocyanine and porphyrin moieties.

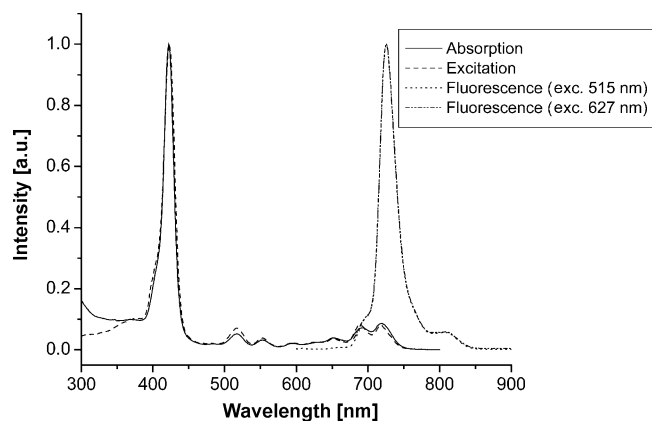


Figure 3. Normalized (B band) electronic absorption, excitation (monitored at 800 nm), and fluorescence spectra ( $\lambda_{\text{exc}} = 515$  nm: Q band of porphyrin moiety, and  $\lambda_{\text{exc}} = 627$  nm: Q band of phthalocyanine moiety) of  $\text{H}_2\text{Pc}-(\text{H}_2\text{TTP})_4$  in toluene (approximately  $1.0 \times 10^{-6}$  M). The two emission spectra coincide completely.

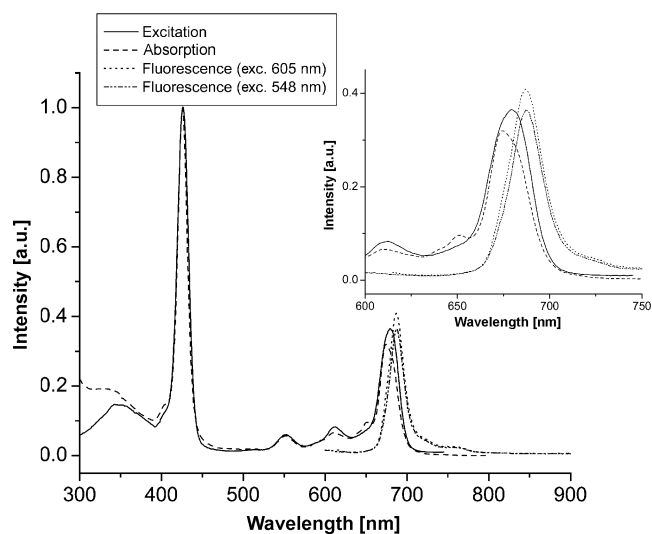


Figure 4. Normalized (B band) electronic absorption, excitation (monitored at 760 nm) and fluorescence spectra ( $\lambda_{\text{exc}} = 548$  nm: porphyrin moiety, and  $\lambda_{\text{exc}} = 605$  nm: phthalocyanine moiety) of  $\text{ZnPc-ZnTTP}$  in toluene (approximately  $1.0 \times 10^{-6}$  M). Inset is an expansion of the Q-band region.

The energy-transfer efficiency can be quantified by analyzing the fluorescence yield of the complex by excitation through the porphyrin moiety and the phthalocyanine moiety separately. Several methods were used to evaluate the energy-transfer efficiency.<sup>[8]</sup> The data in Table 1 were estimated according to a literature method.<sup>[8]</sup> Fluorescence quantum yields of the three compounds were measured to quantify the singlet emission from the phthalocyanine moiety at both wavelengths (Table 1).  $\text{ZnPc}$  ( $\Phi = 0.23$ ),<sup>[13]</sup>  $\text{H}_2\text{Pc}$  ( $\Phi = 0.60$ ),<sup>[14]</sup> and  $\text{H}_2\text{TTP}$  ( $\Phi = 0.11$ )<sup>[15]</sup> were employed as

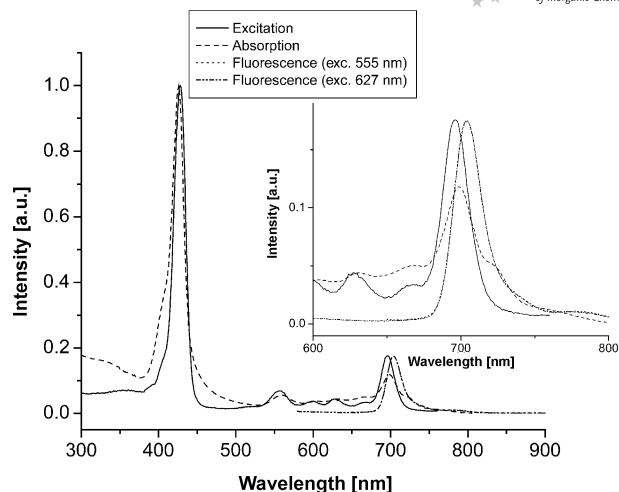


Figure 5. Normalized (B band) electronic absorption, excitation (monitored at 800 nm) and fluorescence spectra ( $\lambda_{\text{exc}} = 555$  nm: porphyrin moiety, and  $\lambda_{\text{exc}} = 627$  nm: phthalocyanine moiety) of  $\text{ZnPc}-(\text{ZnTTP})_4$  in toluene (approximately  $1.0 \times 10^{-6}$  M). The two emission spectra coincide completely.

the reference compounds. The fluorescence quantum yields for all three compounds are exactly the same at both excitation wavelengths corresponding to the porphyrin and phthalocyanine moieties. The fluorescence quantum yield of  $\text{H}_2\text{Pc-H}_2(\text{TTP})_4$  is lower ( $\Phi = 0.30$ ) than that of  $\text{H}_2\text{Pc}$  ( $\Phi = 0.60$ ); for  $\text{ZnPc-ZnTTP}$  and  $\text{ZnPc}-(\text{ZnTTP})_4$ , the fluorescence quantum yields are 0.25 and 0.18, respectively.

Table 1. Photophysical data of the monomers and heteromers in toluene.

Compound	$\lambda_{\text{exc}}$ [nm]	$\tau$ [ns]	$\Phi$	$\Phi_{\text{ET}}$
$\text{H}_2\text{TTP}$	515		0.11	
$\text{H}_2\text{Pc}$	627		0.77	
$\text{ZnPc}$	605		0.23	
$\text{H}_2\text{Pc-H}_2(\text{TTP})_4$	515 <sup>[a]</sup>	6.1	$0.30 \pm 0.02$	$>0.98$
	627 <sup>[b]</sup>		$0.31 \pm 0.02$	
$\text{ZnPc-ZnTTP}$	548 <sup>[a]</sup>	4.5	$0.25 \pm 0.02$	$>0.99$
	605 <sup>[b]</sup>		$0.25 \pm 0.02$	
$\text{ZnPc}-(\text{ZnTTP})_4$	555 <sup>[a]</sup>	6.3	$0.18 \pm 0.02$	$>0.99$
	627 <sup>[b]</sup>		$0.19 \pm 0.02$	

[a] Upon excitation of porphyrin moiety. [b] Upon excitation of phthalocyanine moiety.

## Surface Photovoltaic Properties

Surface photovoltage spectroscopy (SPS) is a useful tool to investigate the photophysics of excited states generated by absorption in the aggregate state,<sup>[16]</sup> since the sensitivity of the method is about  $10^8$  charge/cm<sup>2</sup>, or about one elementary charge per  $10^7$  surface atoms, which exceeds that of conventional spectroscopic methods, such as XPS and Auger spectroscopy, by many orders of magnitude.<sup>[17]</sup> On the basis of the principle of SPS, a field-induced surface photovoltage technique (FISPS)<sup>[18,19]</sup> has been developed to demonstrate the optoelectronic properties of organic semi-



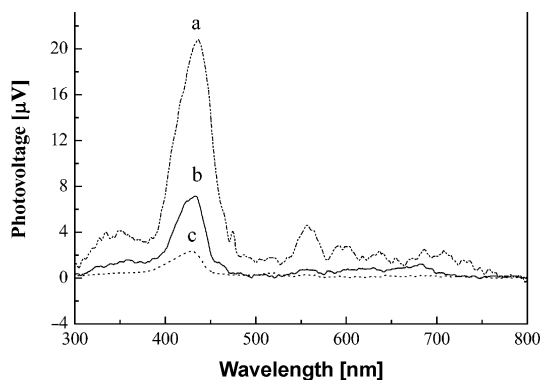


Figure 6. The SPS spectra of (a)  $\text{H}_2\text{Pc}-(\text{H}_2\text{TTP})_4$ , (b)  $\text{ZnTTP}$ , and (c)  $\text{ZnPc}-(\text{ZnTTP})_4$ .

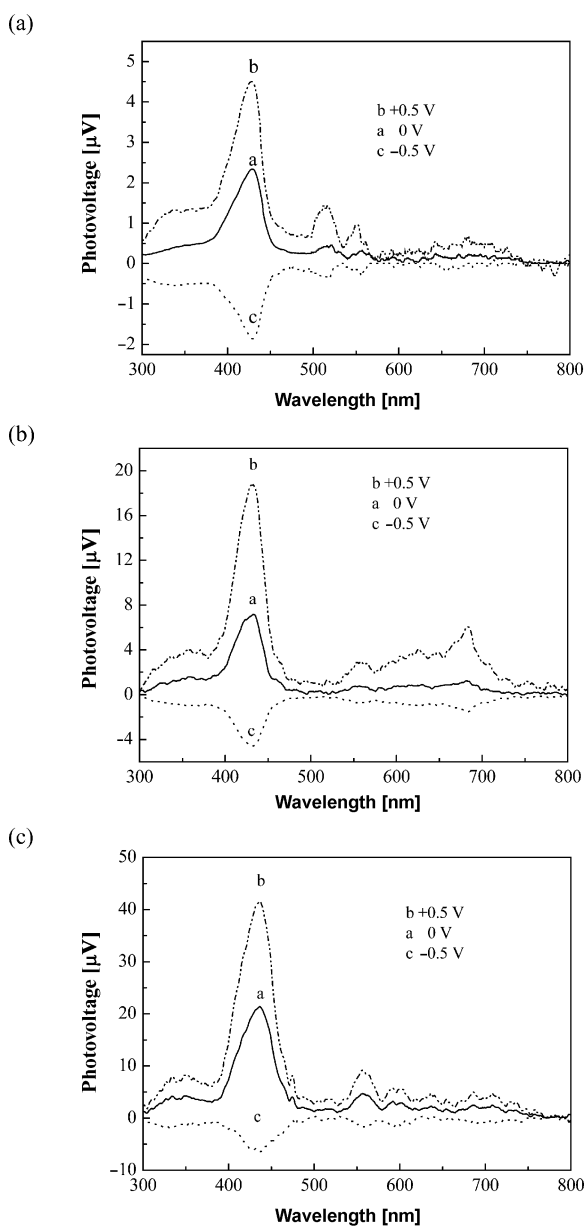


Figure 7. The FISPS of (a)  $\text{ZnPc}-(\text{ZnTTP})_4$ , (b)  $\text{ZnTTP}$ , and (c)  $\text{H}_2\text{Pc}-(\text{H}_2\text{TTP})_4$ .

conductors under the effect of an external electric field.<sup>[20]</sup> By combining SPS with FISPS, one could determine the conduction type of the organic semiconductors. The SPS of  $\text{ZnTTP}$ ,  $\text{ZnPc}-(\text{ZnTTP})_4$ , and  $\text{H}_2\text{Pc}-(\text{H}_2\text{TTP})_4$  are given in Figure 6. It can be seen that the photovoltaic action spectra match the absorption spectral response well, which indicates that the bands correspond to a similar electronic transition. The electrical and photovoltaic properties of solid porphyrins and phthalocyanines have been attributed to the semiconducting behavior of the porphyrins and phthalocyanines themselves. The  $\pi$  orbital is analogous to the valence band of the semiconductor, and the  $\pi^*$  orbital to the conduction band. Photogenerated charge carriers in the  $\pi$  system are nonlocalized, and their motion is free within the energy band of the  $\pi$  system. Photogenerated holes move in the valence band, while photogenerated electrons move in the conduction band. For this kind of system, the band to band transition is characterized as a  $\pi \rightarrow \pi^*$  transition, which is exhibited mainly as Soret B and Q bands. By comparing the SPS data of the three samples, we observe two characteristics. One is that the surface photovoltage (SPV) response intensities of  $\text{H}_2\text{Pc}-(\text{H}_2\text{TTP})_4$  are much larger than those of  $\text{ZnTTP}$  and  $\text{ZnPc}-(\text{ZnTTP})_4$ , which indicates that  $\text{H}_2\text{Pc}-(\text{H}_2\text{TTP})_4$  exhibits a higher photoelectric conversion efficiency. On the other hand, the number of SPV response peaks of the Q band for  $\text{ZnTTP}$  and  $\text{ZnPc}-(\text{ZnTTP})_4$  decreases upon formation of the complexes because the energy band structure and optical constant are changed after metalation. Figure 7 shows the field-induced surface photovoltage spectra (FISPS) of  $\text{ZnTTP}$ ,  $\text{ZnPc}-(\text{ZnTTP})_4$ , and  $\text{H}_2\text{Pc}-(\text{H}_2\text{TTP})_4$ . When a positive field is applied to the irradiated ITO electrode, the SPV response intensities of the three samples are all strikingly enhanced, which demonstrates that the external electric field is of the same sign as that of the built-in field and indicates p-type characteristics of the materials. On the contrary, when a negative electric field is applied, the SPV response intensities are weak and even reversed. Moreover, we note that the B and Q bands of the two samples exhibit a “simultaneous response” with a change in positive or negative electric field intensity. This indicates that they correspond to an analogous transition characteristic, both belonging to the  $\pi \rightarrow \pi^*$  transition. It can also be shown that the variation rate of B and Q bands differs with a change in positive or negative electric field because of the differing separation of the lower energy levels from the valence band for these transitions.

### Electrochemistry

The redox properties of  $\text{H}_2\text{Pc}-(\text{H}_2\text{TTP})_4$ ,  $\text{ZnPc}-(\text{ZnTTP})_4$ , and  $\text{ZnTTP}$  were studied by cyclic voltammetry in  $\text{CH}_2\text{Cl}_2$  containing  $\text{NBu}_4\text{PF}_6$ . Table 2 presents the potential values in each case at room temperature. The metal-free compound  $\text{H}_2\text{Pc}-(\text{H}_2\text{TTP})_4$  displays an irreversible anodic wave and two reversible reduction waves typical of ring-based processes. The separation between the first and second ring reductions in  $\text{H}_2\text{Pc}-(\text{H}_2\text{TTP})_4$  was found to be

within the range reported for ring-based reductions in some nontransition-metal phthalocyanines.<sup>[21]</sup> ZnPc–ZnTTP and ZnPc–(ZnTTP)<sub>4</sub> show a reversible oxidation wave at 0.29 and 0.04 V, respectively, and both these processes are ring-based since the central Zn metal is electroinactive. Metalation of H<sub>2</sub>Pc–(H<sub>2</sub>TTP)<sub>4</sub> by Zn<sup>2+</sup> induces a cathodic shift in the reduction potential from –1.91 to –2.15 V. Displacement of the two protons in the inner porphyrin or phthalocyanine core with a metal ion leads to a shift in the first ring-based reduction potential to a more negative value as a result of the  $\pi$  back donation of the filled  $d\pi$  orbital of the metal ion into the empty porphyrin or phthalocyanine  $\pi^*$  orbitals.<sup>[10b]</sup>

Table 2. Electrochemical data for H<sub>2</sub>Pc–(H<sub>2</sub>TTP)<sub>4</sub>, ZnPc–ZnTTP, and ZnPc–(ZnTTP)<sub>4</sub>.<sup>[a]</sup>

	$E_{\text{ox}}$ [V]	$E_{\text{red}}$ [V]
H <sub>2</sub> Pc–(H <sub>2</sub> TTP) <sub>4</sub>	0.33 (i)	–1.91 (r), –2.25 (r)
ZnPc–ZnTTP	0.29 (r)	–1.30 (r), –1.93 (r)
ZnPc–(ZnTTP) <sub>4</sub>	0.04 (r)	–2.15 (r)

[a] i = irreversible wave; r = reversible wave.

### Optical-Power-Limiting Properties

Optical limiters are devices that can protect sensitive optical sensors against high optical power. In other words, these devices limit the transmitted intensity of a bright optical beam to some specified maximum (ideally to a safe level without causing damage to the eye or optical sensor) but exhibits high transmittance for low-intensity ambient light levels. The optical-power-limiting (OPL) effect can be explained by a mechanism known as reverse saturable absorption (RSA).<sup>[22]</sup> So far, metallophthalocyanine and metallocporphyrins continue to attract considerable attention because the structure–property relationships can be investigated easily through structural modification by changing the central metal center and ligand substituents.<sup>[23]</sup> We therefore studied the OPL effect of our phthalocyanine–porphyrin heterodimer and pentamer. The intensity-dependent transmittance and Z-scan measurements were performed with Ti:Sapphire laser with an output wavelength of 400 and 800 nm. From the Z-scan curves for the three complexes measured in CHCl<sub>3</sub> (Figure 8), all of the complexes show excellent OPL behavior at both 400 and 800 nm excitation. It is clear that the complex ZnPc–ZnTTP shows the strongest OPL capability at 400 nm excitation, whereas H<sub>2</sub>Pc–(H<sub>2</sub>TTP)<sub>4</sub> gives the strongest response at 800 nm excitation. Both of them have an OPL performance that is comparable to that of the benchmark material C<sub>60</sub>. At 400 nm, the transmittance for H<sub>2</sub>Pc–(H<sub>2</sub>TTP)<sub>4</sub>, ZnPc–ZnTTP, and ZnTTP–(ZnTTP)<sub>4</sub> decreases to 52%, 48%, and 49% of their original linear transmission, respectively (cf. 58% for C<sub>60</sub>, see Figure 8a). The corresponding transmittance values drop to 13%, 23%, and 37%, respectively, at 800 nm (cf. 17% for C<sub>60</sub>, see Figure 8b). The performance of these reverse saturable absorbers can also be compared quantitatively by using the figure of merit factor  $\delta_{\text{eff}}/\delta_0$ , where  $\delta_{\text{eff}}$

and  $\delta_0$  are the effective excited-state and ground-state absorption cross sections, respectively.<sup>[24]</sup> RSA occurs when the cross section of the excited state is larger than that of the ground state. It was observed that our compounds show OPL behavior with good  $\delta_{\text{eff}}/\delta_0$  values (9.94, 11.09, and 10.73 for H<sub>2</sub>Pc–(H<sub>2</sub>TTP)<sub>4</sub>, ZnPc–ZnTTP, and ZnTTP–(ZnTTP)<sub>4</sub>, respectively), which slightly exceed or are at least comparable to that of C<sub>60</sub> (9.06).

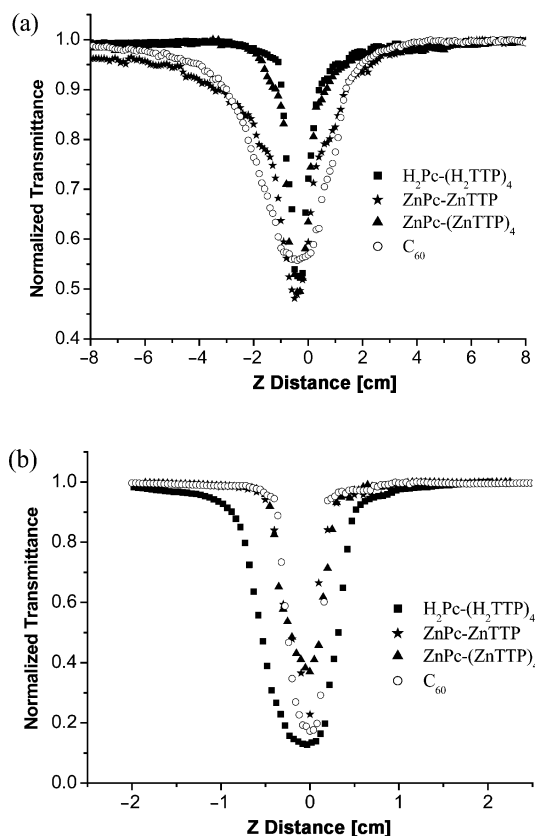


Figure 8. Open aperture Z-scans for optical-limiting measurements at the linear transmittance of 93% at (a) 400 nm and (b) 800 nm.

### Conclusions

Nonperipherally substituted porphyrin–phthalocyanine light-harvesting arrays have been prepared by cyclotetramerization of substituted phthalonitriles, which are effective light harvesters and optical power limiters. The porphyrins are especially efficient at transferring energy to phthalocyanines upon excitation at their B or Q bands. The phthalocyanine moieties are also good acceptors of energy and their photophysical properties can be modified greatly by the presence of a porphyrin on its nonperiphery.

### Experimental Section

**Materials:** All reactions were carried out under an atmosphere of dry nitrogen. The chemicals were purchased from Sigma–Aldrich and used without further purification. 3-Iodophthalonitrile,<sup>[11]</sup> 4-

ethynylbenzaldehyde and SubPc<sup>[25]</sup> were synthesized as published. All solvents were dried by the standard methods prior to use. Silica gel 60 (0.04–0.063 mm) for column chromatography was purchased from Merck. The IR spectra (KBr pellets) were recorded with a Nicolet Nagba-IR 550 spectrometer and NMR spectra with a Varian INOVA 400 spectrometer. Electrospray ionization high-resolution mass spectra (ESI-HRMS) were recorded with a QSTAR mass spectrometer. Electronic absorption spectra in the UV/Vis region were recorded with a Hewlett–Packard 8453 UV/Vis spectrophotometer, steady-state visible fluorescence and PL excitation spectra with a Photon Technology International (PTI) Alphascan spectrofluorimeter, and visible decay spectra with a pico-N<sub>2</sub> laser system (PTI Time Master) with  $\lambda_{\text{exc}} = 337$  nm. Electrochemical measurements were made in CH<sub>2</sub>Cl<sub>2</sub> by using a Princeton Applied Research (PAR) model 273A potentiostat. A conventional three-electrode configuration consisting of a glassy-carbon working electrode, and Pt wires as both the counter and reference electrodes were used. The supporting electrolyte was 0.1 M [Bu<sub>4</sub>N]PF<sub>6</sub>. Ferrocene was added as a calibrant after each set of measurements, and all potentials reported were quoted with reference to the ferrocene/ferrocenium (Fc/Fc<sup>+</sup>) couple at a scan rate of 100 mV s<sup>−1</sup>. Surface photovoltage spectra (SPS) were measured with a solid junction photovoltaic cell (ITO/porphyrin films/ITO) by using light-source-monochromator-lock-in detection technique. The principle and setup diagram of SPS and field-induced surface photovoltage spectroscopic (FISPS) measurements have already been described in detail elsewhere.<sup>[26]</sup> The measurement was performed under atmospheric pressure and at ambient temperature (about 20 ± 2 °C). The investigation of the optical-limiting properties was performed with a mode-locked Ti:Sapphire laser (Spectra Physics – Tsunami) and Ti:Sapphire amplifier (Spectra Physics – Spitfire) at the repetition of 1 kHz. The laser was frequency doubled with an output wavelength of 400 or 800 nm with a 100-fs pulse width for Gaussian mode by a frequency double crystal (FDC). The laser beam was then split into two beams by a beam splitter (BS). One was used as the reference beam, which was received by a detector (D<sub>1</sub>), the other was for the sample measurement and it was focused with a lens (L<sub>1</sub>,  $f = 20$  cm). After transmittance of the light beam through the sample (S), it entered another detector (D<sub>2</sub>). The sample to be measured was moved along a rail to change the incidence irradiance on it. The incident and transmitted energies were detected simultaneously by the two detectors D<sub>1</sub> and D<sub>2</sub> (LPE-1A) individually. The solution samples were measured in a 1-mm quartz cell.

## Synthesis

**4-[2-(2,3-Dicyanophenyl)ethynyl]benzaldehyde:** 3-Iodophthalonitrile (1.78 g, 7.01 mmol), 4-ethynylbenzaldehyde (1.18 g, 7.01 mmol), Pd(PPh<sub>3</sub>)<sub>2</sub>Cl<sub>2</sub> (98.1 mg, 0.14 mmol), and CuI (53.4 mg, 0.28 mmol) were added to a mixture of deaerated triethylamine (15 mL) and THF (10 mL) under nitrogen. The mixture was stirred overnight, and then the solvent was removed by distillation under reduced pressure. Chloroform (100 mL) was added to the yellow product, which was washed three times with 5% NaHCO<sub>3</sub> solution. The chloroform layer was collected, solvents evaporated, and the yellow solid applied to a silica gel column. The desired compound was eluted as the third band by using chloroform/hexane (3:1, v/v), which after removal of the solvent, afforded a pale yellow solid in 78% yield (1.40 g). <sup>1</sup>H NMR (400 MHz, CDCl<sub>3</sub>):  $\delta = 7.74$ – $7.80$  (m, 4 H, phenyl H),  $7.87$ – $7.94$  (m, 3 H, phenyl H),  $10.06$  (s, 1 H, CHO) ppm. IR (KBr, in):  $\tilde{\nu} = 2212$  (CN),  $1696$  (CO) cm<sup>−1</sup>. ESI for C<sub>17</sub>H<sub>8</sub>N<sub>2</sub>O (256.3): calcd. for [M + Na]<sup>+</sup> 279.0529; found 279.0548.

**5,10,15-Tritolyl-20-{4-[2-(2,3-dicyanophenyl)ethynyl]phenyl}-porphyrin (H<sub>2</sub>CNTTP):** Samples of *p*-tolualdehyde (0.18 mL,

0.50 mmol), 4-[2-(2,3-dicyanophenyl)ethynyl]benzaldehyde (128 mg, 0.50 mmol), and pyrrole (0.14 mL, 20 mmol) were condensed in CH<sub>2</sub>Cl<sub>2</sub> (200 mL) with BF<sub>3</sub>·OEt<sub>2</sub> (0.266 mL of a 2.5 M stock solution in CH<sub>2</sub>Cl<sub>2</sub>, 0.665 mmol) at room temperature for 1 h. Then DDQ (342 mg, 1.50 mmol) was added and stirring was continued at room temperature for a further 1 h. Flash chromatography (Al<sub>2</sub>O<sub>3</sub>) was applied to remove non-porphyrinic components from the crude reaction mixture. Column chromatography on silica gel with CH<sub>2</sub>Cl<sub>2</sub>/hexane (3:1, v/v) as eluent gave the desired product as the second red band. Evaporation of the solvent afforded a purple solid (61 mg, 15%). The purple crude product was recrystallized from CH<sub>2</sub>Cl<sub>2</sub>/methanol. UV/Vis (toluene):  $\lambda_{\text{max}}$  (log  $\epsilon$ ) = 422 (5.71), 517 (4.26), 552 (4.03), 593 (3.74), 649 (3.71) nm. <sup>1</sup>H NMR (400 MHz, CDCl<sub>3</sub>):  $\delta = -2.78$  (s, 2 H, N–H), 2.71 (s, 9 H, CH<sub>3</sub>), 7.54 (d,  $J = 8.0$  Hz, 6 H, phenyl H), 7.74–8.05 (m, 3 H, phthalonitrile H), 8.03 (d,  $J = 8.0$  Hz, 6 H, phenyl H), 8.10 (d,  $J = 8.0$  Hz, 2 H, phenyl H), 8.80–8.90 (m, 8 H, pyrrole H) ppm. IR (KBr, in):  $\tilde{\nu} = 3316$  (N–H), 2918 (CH), 2217 (CN), 1581, 1473, 1399, 1349, 1219, 1181, 982, 966, 799, 734 cm<sup>−1</sup>. MALDI-TOF-MS for C<sub>57</sub>H<sub>38</sub>N<sub>6</sub> (807.0): calcd. for [M + H]<sup>+</sup> 807.3231; found 807.3262.

**5,10,15-Tritolyl-20-{4-[2-(2,3-dicyanophenyl)ethynyl]phenyl}-porphyrin Zinc(II) (ZnCNTTP):** A mixture of H<sub>2</sub>CNTTP (40 mg, 0.05 mmol) and Zn(OAc)<sub>2</sub>·2H<sub>2</sub>O (10.8 mg, 0.05 mmol) in CHCl<sub>3</sub> (10 mL) and methanol (10 mL) was stirred at room temperature for 12 h. After removal of the solvent, the solid was dissolved in a minimum volume of CHCl<sub>3</sub> and loaded onto a silica gel column. Elution with CHCl<sub>3</sub>/hexane (3:1, v/v) afforded one vivid red band only. Removal of chloroform by evaporation afforded the product in an almost quantitative yield (42 mg, 98%). UV/Vis (toluene):  $\lambda_{\text{max}}$  (log  $\epsilon$ ) = 426 (5.67), 551 (4.35), 591 (3.81) nm. <sup>1</sup>H NMR (400 MHz, CDCl<sub>3</sub>):  $\delta = 2.71$  (s, 9 H, CH<sub>3</sub>), 7.54 (d,  $J = 7.6$  Hz, 6 H, phenyl H), 7.75–8.03 (m, 3 H, phthalonitrile H), 8.08 (d,  $J = 7.6$  Hz, 6 H, phenyl H), 8.25 (d,  $J = 7.6$  Hz, 2 H, phenyl H), 8.90–8.99 (m, 8 H, pyrrole H) ppm. IR (KBr, in):  $\tilde{\nu} = 2212$  (CN), 2921 (CH), 1583, 494, 1339, 1205, 1180, 1000, 797, 721 cm<sup>−1</sup>. MALDI-TOF-MS for C<sub>57</sub>H<sub>38</sub>N<sub>6</sub>Zn (870.0): calcd. for [M + H]<sup>+</sup> 868.2292; found 868.2247.

**All-Free-Base Heteropentamer [H<sub>2</sub>Pc-(H<sub>2</sub>TTP)<sub>4</sub>]:** To 1-pentanol (10 mL) was added lithium ribbon (147.1 mg, 21 mmol). The mixture was stirred under nitrogen at 90 °C for 3 h until all of the lithium was consumed. After cooling of the mixture to room temperature, H<sub>2</sub>CNTTP (170 mg, 0.21 mmol) was added. The reaction mixture was then heated to 145 °C and stirred under nitrogen for 4 h. The solvent was removed by vacuum. Chloroform (100 mL) was added and washed three times with water (100 mL). The chloroform layer was collected, solvents evaporated, and the solid applied to a silica gel column. Elution with CHCl<sub>3</sub>/methanol (50:1, v/v) afforded a green-brown band. Removal of the solvent by evaporation afforded a purple solid (61.2 mg, 36%). The purple product was recrystallized from a mixture of chloroform and hexane. UV/Vis (CHCl<sub>3</sub>):  $\lambda_{\text{max}}$  (log  $\epsilon$ ) = 422 (6.09), 517 (4.79), 554 (4.59), 594 (4.40), 650 (4.57), 687 (4.85), 718 (4.91) nm. <sup>1</sup>H NMR (400 MHz, CDCl<sub>3</sub>):  $\delta = 9.15$  (br. s, 4 H, phthalocyanine H), 8.52–8.90 (m, 32 H, pyrrole H), 8.33–8.50 (br. s, 8 H, phenyl H), 7.90–8.20 (br. s, 24 H, phenyl H), 7.46–7.76 (br. d, 32 H, phenyl H), 6.81–7.07 (br. s, 8 H, phthalocyanine H), 2.71 (s, 36 H, CH<sub>3</sub>), −2.79 (br. s, 8 H, N–H) ppm. IR (KBr, in):  $\tilde{\nu} = 3312$  (NH), 2910, 1502, 1469, 1347, 1220, 1182, 1102, 1023, 965, 798, 731 cm<sup>−1</sup>. MALDI-TOF-MS for C<sub>228</sub>H<sub>154</sub>N<sub>24</sub> (3229.8): calcd. for [M + H]<sup>+</sup> 3230.2924; found 3230.2765.

**All-Zinc Heteropentamer [ZnPc-(ZnTTP)<sub>4</sub>]:** To 1-pentanol (10 mL) was added lithium ribbon (83 mg, 12 mmol). The mixture was



stirred at 90 °C until all of the lithium was consumed. At this point, the alkoxide solution was cooled to room temperature, and ZnCNTTP (130 mg, 0.15 mmol) was added. The reaction mixture was then heated to 145 °C and stirred under nitrogen for 4 h. The temperature was then lowered to 80 °C, and Zn(OAc)<sub>2</sub>·2H<sub>2</sub>O (329.3 mg, 1.5 mmol) was added. The reaction mixture was allowed to stir for an additional 4 h at 80 °C. The reaction mixture was then cooled to room temperature. Chloroform (100 mL) was added, and the chloroform layer was washed with water (3 × 100 mL). The chloroform layer was collected, concentrated under vacuum, and loaded onto a silica gel column. Elution with chloroform afforded the desired product from the second green-brown band. Removal of the solvent by evaporation afforded a purple solid (46.5 mg, 35%). The purple product was recrystallized from CHCl<sub>3</sub>/hexane. UV/Vis (CHCl<sub>3</sub>): λ<sub>max</sub> (log ε) = 426 (6.11), 558 (4.86), 603 (4.70), 628 (4.76), 695 (5.19) nm. <sup>1</sup>H NMR (400 MHz, CDCl<sub>3</sub>): δ = 9.18 (br. s, 4 H, phthalocyanine H), 8.87–9.05 (br. m, 32 H, pyrrole H), 7.92–8.23 (br. s, 32 H, phenyl H), 7.39–7.66 (br. m, 32 H, phenyl H), 7.03–7.18 (br. s, 4 H, phthalocyanine H), 7.85–7.00 (br. s, 4 H, phthalocyanine H), 2.68 (s, 36 H, CH<sub>3</sub>) ppm. IR (KBr, in): ν̄ = 2923 (CH), 1731, 1633, 1457, 1337, 1205, 1110, 1067, 997, 797, 720 cm<sup>−1</sup>. MALDI-TOF-MS for C<sub>228</sub>H<sub>154</sub>N<sub>24</sub>Zn<sub>5</sub> (3546.7): calcd. for [M + H]<sup>+</sup> 3546.8530; found 3546.8359.

**Zinc Heterodimer [ZnPc–ZnTTP]:** SubPc (216 mg, 0.5 mmol) in DMSO (10 mL) was heated to 60 °C for 2 h while stirring under nitrogen. ZnCNTTP (86.7 mg, 0.10 mmol), DBU (2 drops), and hydrated zinc acetate (108 mg, 0.50 mmol) were added to the solution. The mixture was heated to 120 °C for 24 h while stirring under nitrogen. After cooling to room temperature, the green reaction mixture was poured into dichloromethane (100 mL) and washed with water (3 × 100 mL) to remove excess zinc acetate, acetic acid, and DMSO. The dichloromethane layer was collected and concentrated which was then applied to a silica gel column. The blue band consisting of the desired compound was eluted by using a mixture of dichloromethane and methanol (95:5, v/v). The by-product ZnPc remained on the top of the column. Removal of the solvents by evaporation afforded a purple solid (36.9 mg, 28%). The purple product ZnPc–ZnTTP was recrystallized from CH<sub>2</sub>Cl<sub>2</sub>/methanol. UV/Vis (CHCl<sub>3</sub>): λ<sub>max</sub> (log ε) = 426 (5.95), 555 (4.67), 610 (4.80), 652 (4.93), 676 (5.47) nm. <sup>1</sup>H NMR (400 MHz, [D<sub>6</sub>]DMSO): δ = 9.28 (br. s, 4 H, phthalocyanine H), 9.10 (br. s, 1 H, phthalocyanine H), 9.00 (br. s, 1 H, phthalocyanine H), 8.68–8.87 (br. m, 8 H, pyrrole H), 8.47–8.65 (br. m, 2 H, phenyl H), 7.98–8.28 (br. m, 12 H, phenyl and phthalocyanine H), 7.50–7.70 (br. m, 8 H, phenyl H), 2.67 (s, 9 H, CH<sub>3</sub>) ppm. IR (KBr, in): ν̄ = 2923, 1722, 1486, 1464, 1332, 1093, 997, 797, 721 cm<sup>−1</sup>. FAB-MS: m/z = 1320.3 [M]<sup>+</sup>. MALDI-TOF-MS for C<sub>81</sub>H<sub>48</sub>N<sub>12</sub>Zn<sub>2</sub> (1320.1): calcd. for [M]<sup>+</sup> 1320.2683; found 1320.2710.

## Acknowledgments

The work described in this paper was partially supported by a grant from the Research Grants Council of the Hong Kong Special Administrative Region, P.R. China (HKBU 2023/04P) and a grant from the Hong Kong Baptist University (FRG/03–04/II-05).

- [1] a) G. J. Meyer in *Progress in Inorganic Chemistry, Molecular Level Artificial Photosynthetic Materials*, vol. 44, Jossey-Bass, New York, **1996**; b) R. W. Wagner, J. S. Lindsey, *J. Am. Chem. Soc.* **1994**, *116*, 9759–9760.
- [2] M. S. Xu, J. B. Xu, M. Wang, L. Que, *J. Appl. Phys.* **2002**, *91*, 748–752.

- [3] D. Gu, O. Chen, X. Tang, F. Tang, F. Gan, S. Shen, K. Liu, H. Xu, *Proc. SPIE-Int. Soc. Opt. Eng.* **1996**, *2931*, 67–72.
- [4] L. E. Norena-Franco, F. Kvasnik, *Analyst* **1996**, *121*, 1115–1118.
- [5] A. M. Hagfeldt, *Acc. Chem. Res.* **2000**, *33*, 269–277.
- [6] S. L. Haywood-Small, D. I. Vernon, J. Griffiths, S. B. Brown, *Biochem. Biophys. Res. Commun.* **2006**, *339*, 569–576.
- [7] S. Gaspard, C. Giannotti, P. Maillard, C. Schaeffer, T. H. Tran-Thi, *J. Chem. Soc., Chem. Commun.* **1986**, 1239–1240.
- [8] a) J.-Z. Li, J. R. Diers, J. Seth, S. I. Yang, D. F. Bocian, D. Holten, J. S. Lindsey, *J. Org. Chem.* **1999**, *64*, 9090–9100; b) J.-Z. Li, J. S. Lindsey, *J. Org. Chem.* **1999**, *64*, 9101–9108; c) S. I. Yang, J.-Z. Li, H. S. Cho, D. Kim, D. F. Bocian, D. Holten, J. S. Lindsey, *J. Mater. Chem.* **2000**, *10*, 283–296; d) M. A. Miller, R. K. Lammi, S. Prathapan, D. Holten, J. S. Lindsey, *J. Org. Chem.* **2000**, *65*, 6634–6649.
- [9] a) J. M. Sutton, R. W. Boyle, *Chem. Commun.* **2001**, 2014–2015; b) K. Kameyama, A. Satake, Y. Kobuke, *Tetrahedron Lett.* **2004**, *45*, 7617–7620; c) J. P. C. Tomé, A. M. V. M. Pereira, C. M. A. Alonso, M. G. P. M. S. Neves, A. C. Tomé, A. M. S. Silva, J. A. S. Cavaleiro, M. V. Martínez-Díaz, T. Torres, G. M. A. Rahman, J. Ramey, D. M. Guldi, *Eur. J. Org. Chem.* **2006**, 257–267.
- [10] a) Z.-X. Zhao, A. O. Ogunsipe, M. D. Maree, T. Nyokong, *J. Porphyrins Phthalocyanines* **2005**, *9*, 186–197; b) Z.-X. Zhao, K. I. Ozoemena, D. M. Maree, T. Nyokong, *Dalton Trans.* **2005**, 1241–1248; c) K. I. Ozoemena, Z.-X. Zhao, T. Nyokong, *Electrochem. Commun.* **2005**, *7*, 679–684; d) Z.-X. Zhao, T. Nyokong, M. D. Maree, *Dalton Trans.* **2005**, 3732–3737.
- [11] A. A. Pletnev, Q.-P. Tian, R. C. Larock, *J. Org. Chem.* **2002**, *67*, 9276–9287.
- [12] J. Metz, O. Schneider, M. Hanack, *Inorg. Chem.* **1984**, *23*, 1065–1071.
- [13] T. H. Tran-Thi, C. Desforge, C. Thiec, *J. Phys. Chem.* **1989**, *93*, 1226–1233.
- [14] P. G. Seybold, M. Gouterman, *J. Mol. Spectrosc.* **1969**, *31*, 1–13.
- [15] K. Kalyanasundaram, *Photochemistry of Polypyridine and Porphyrin Complexes*, Academic Press, London, **1992**.
- [16] A. Köhler, J. Grüner, R. H. Friend, K. Mullen, U. Scherf, *Chem. Phys. Lett.* **1995**, *243*, 456–461.
- [17] H. C. Gatos, J. Lagowski, R. Banisch, *Photogr. Sci. Eng.* **1982**, *26*, 42–49.
- [18] J. Zhang, D. J. Wang, T. S. Shi, B. H. Wang, J. Z. Sun, T. J. Li, *Thin Solid Films* **1996**, *284/285*, 596–599.
- [19] J. Zhang, D. J. Wang, Y. M. Chen, T. J. Li, H. F. Mao, H. J. Tian, Q. F. Zhou, H. J. Xu, *Thin Solid Films* **1997**, *300*, 208–212.
- [20] D. J. Wang, J. Zhang, T. S. Shi, B. H. Wang, X. Z. Cao, T. J. Li, *J. Photochem. Photobiol., A* **1996**, *93*, 21–25.
- [21] a) P. Matlaba, T. Nyokong, *Polyhedron* **2002**, *21*, 2463; b) A. B. P. Lever, E. R. Milaeva, G. Speier, *Phthalocyanines: Properties and Applications*, C. C. Leznoff, A. B. P. Lever (Eds.), vol. 3, ch. 1, VCH, New York, **1993**.
- [22] a) D. G. Mclean, R. L. Sutherland, M. C. Brant, D. M. Brandelik, *Opt. Lett.* **1993**, *18*, 858–860; b) S. Fu, X. Zhu, G. Zhou, W.-Y. Wong, C. Ye, W.-K. Wong, Z. Li, *Eur. J. Inorg. Chem.* **2007**, 2004–2013.
- [23] a) X. Zhong, Y. Feng, S.-L. Ong, J. Hu, W.-J. Ng, Z. Wang, *Chem. Commun.* **2003**, 1882–1883; b) A. Krivokapic, H. L. Anderson, G. Bourhill, R. Ives, S. Clark, K. J. McEwan, *Adv. Mater.* **2001**, *13*, 652–656; c) G. Y. Yang, S. G. Ang, L. L. Chng, Y. W. Lee, E. W.-P. Lau, K. S. Lai, H. G. Ang, *Chem. Eur. J.* **2003**, *9*, 900–904; d) S. Vagin, M. Barthel, D. Dini, M. Hanack, *Inorg. Chem.* **2003**, *42*, 2683–2694; e) R. B. Martin, H. Li, L. Gu, S. Kumar, C. M. Sanders, Y.-P. Sun, *Opt. Mater.* **2005**, *27*, 1340–1345; f) S. Fu, G. Zhou, X. Zhu, C. Ye, W. K. Wong, Z. Li, *Chem. Lett.* **2006**, *35*, 802–803; g) J. W. Perry, K. Mansour, I.-Y. S. Lee, X.-L. Wu, P. V. Bedworth, C.-T. Chen, D. Ng, S. Marder, P. Miles, *Science* **1996**, *273*, 1533–1536; h) J. W. Perry,

- K. Mansour, S. R. Marder, K. J. Perry, D. Alvarez Jr, I. Choong, *Opt. Lett.* **1994**, *19*, 625–627.
- [24] a) G.-J. Zhou, W.-Y. Wong, Z. Lin, C. Ye, *Angew. Chem. Int. Ed.* **2006**, *45*, 6189–6193; b) G.-J. Zhou, W.-Y. Wong, C. Ye, Z. Lin, *Adv. Funct. Mater.* **2007**, *17*, 963–975.
- [25] a) D. Gonzalez-Rodriguez, C. G. Claessens, T. Torres, S.-G. Liu, L. Echegoyen, N. Vila, S. Nonell, *Chem. Eur. J.* **2005**, *11*, 3881–3893; b) C. G. Claessens, T. Torres, *Chem. Eur. J.* **2000**, *6*, 2168–2172.
- [26] a) D. J. Wang, J. Zhang, T. S. Shi, B. H. Wang, X. Z. Cao, T. J. Li, *J. Photochem. Photobiol., A* **1996**, *93*, 21–25; b) T. F. Xie, D. J. Wang, L. J. Zhu, C. Wang, T. J. Li, X. Q. Zhou, M. Wang, *J. Phys. Chem. B* **2000**, *104*, 8177–8181.

Received: July 10, 2007

Published Online: November 8, 2007